Hydrostatic Pressure Induces Hydrocarbon Chain Interdigitation in Single-Component Phospholipid Bilayers

Lellis F. Braganza* and David L. Worcester‡

Institut Laue-Langevin, 156X, 38042 Grenoble Cedex, France

Received August 12, 1985; Revised Manuscript Received November 21, 1985

ABSTRACT: By use of neutron diffraction for structural analysis, the temperature–pressure phase diagrams of several fully hydrated single-component phospholipid bilayers have been explored up to hydrostatic pressures of 2 kbars. The gel to liquid-crystalline phase transition temperature T_m increases linearly with pressure over a 10^{-3}–2 kbar range in accordance with the Clausius–Clapeyron relationship giving dT_m/dP values of 23.0 °C/kbar for 1,2-dimyristoyl-*sn*-glycero-3-phosphatidylcholine (DMPC) and 1,2-dipalmitoyl-*sn*-glycero-3-phosphatidylcholine (DPPC) and 28.0 °C/kbar for 1,2-distearoyl-*sn*-glycero-3-phosphatidylcholine (DSPC). The so-called pretransition was not observed in the isothermal pressure experiments, suggesting that no appreciable volume change occurs at this transition. These results are in good agreement with those reported using other techniques. In addition, at pressures higher than the isothermal liquid-crystalline to gel transition pressure, a new pressure-induced phase transition was observed for DPPC and DSPC in which the hydrocarbon chains from apposing monolayers become interdigitated with the chains occupying a cross-sectional area $\simeq 5\%$ less than in the gel phase. The temperature–pressure phase diagrams show the gel-interdigitated phase boundaries to be highly curved and the minimum pressure at which interdigitation occurs to decrease with increasing hydrocarbon chain length.

Hydrostatic pressure acts so as to decrease the total volume of a system at equilibrium and has proved to be a valuable thermodynamic variable in the study of chemical and physical processes which occur in liquids and solutions (Weber & Drickamer, 1983). Solids and liquids have relatively low compressibilities that are determined by interatomic or intermolecular forces and range from $\simeq 10^{-3}$/kbar for metals to 10^{-1}/kbar for simple alcohols such as methanol. In contrast, chemical equilibria in solution often involve much larger volume changes due to different intermolecular forces of the solvated products and reactants. One important example is the separation of ion pairs which usually results in a large volume decrease due to the "electrostriction" of water around ionic charges (e.g., $CH_3COOH + H_2O \rightleftharpoons H_3O^+ + CH_3COO^-$, $\Delta V \simeq -10$ cm^3 mol^{-1}) (Lown et al., 1968) and is strongly influenced by pressure if the equilibrium is near the midpoint or "poised". Another is the observation that the molar volumes of hydrocarbons in dilute aqueous solution are smaller than in nonpolar solvents (Masterton, 1954), suggesting that pressure would promote the aqueous solvation of hydrophobic molecules.

Recently, we have used neutron diffraction together with hydrostatic pressure and temperature to study interactions between the ordered membrane layers of nerve myelin (D. L. Worcester and L. F. Braganza, unpublished results). In order to separate the effects of pressure on reactions which occur in the aqueous interface between myelin membranes from changes in the membrane hydrocarbon region, we have carried out similar studies on synthetic, phospholipid multilamellar vesicle (MLV)[1] dispersions and oriented multilayers. The results of some of these model membrane studies are reported here.

Because of the large difference in coherent neutron-scattering amplitudes of hydrogen and deuterium, the bilayer surfaces can be clearly located in Fourier profiles obtained by using the lamellar diffraction from oriented multilayers of phosphatidylcholines with deuteriocarbon chains and protonated head groups. Wide-angle diffraction from the deuteriocarbon chains was also measured and enabled the interchain spacing to be determined, so that both changes in bilayer thickness and chain spacing have been directly measured as a function of hydrostatic pressure and temperature. Lipid-phase changes were determined from changes in the neutron diffraction patterns.

The effect of pressure on the gel to liquid-crystalline phase transition temperature, T_m, of synthetic phospholipids has previously been investigated by a variety of methods including ESR (Trudell et al., 1974), volumetry (Liu & Kay, 1977), light scattering (Ceuterick et al., 1978), calorimetry (Mountcastle et al., 1978), and steady-state polarization fluorometry (Chong & Weber, 1983). These measurements show that T_m increases linearly with hydrostatic pressure in accordance with the Clausius–Clapeyron relationship, giving values of dT_m/dP in the range 15–30 °C/kbar. In addition to the isothermal pressure induced liquid-crystalline to gel transition for DPPC and DSPC, we find an interdigitated hydrocarbon phase occurring at higher pressures and that the pressure at which this transition takes place varies nonlinearly with temperature.

Materials and Methods

Materials. 1,2-Dimyristoyl-*sn*-glycero-3-phosphatidylcholine (DMPC), 1,2-dipalmitoyl-*sn*-glycero-3-phosphatidylcholine (DPPC), and 1,2-distearoyl-*sn*-glycero-3-phosphatidylcholine (DSPC) were purchased from Fluka AG, CH-9470 Buchs, Switzerland (puriss grade $\simeq 99\%$ pure), and used without further purification. DPPC with deuteriocarbon chains was obtained from Lipid Specialities Inc., Boston, MA.

‡Present address: Biology Division and Intense Pulsed Neutron Source (IPNS), Argonne National Laboratory, Argonne, IL 60439.

[1] Abbreviations: DMPC, 1,2-dimyristoyl-*sn*-glycero-3-phosphatidylcholine; DPPC, 1,2-dipalmitoyl-*sn*-glycero-3-phosphatidylcholine; DSPC, 1,2-distearoyl-*sn*-glycero-3-phosphatidylcholine; ESR, electron spin resonance; MLVs, multilamellar lipid vesicles.

0006-2960/86/0425-2591$01.50/0

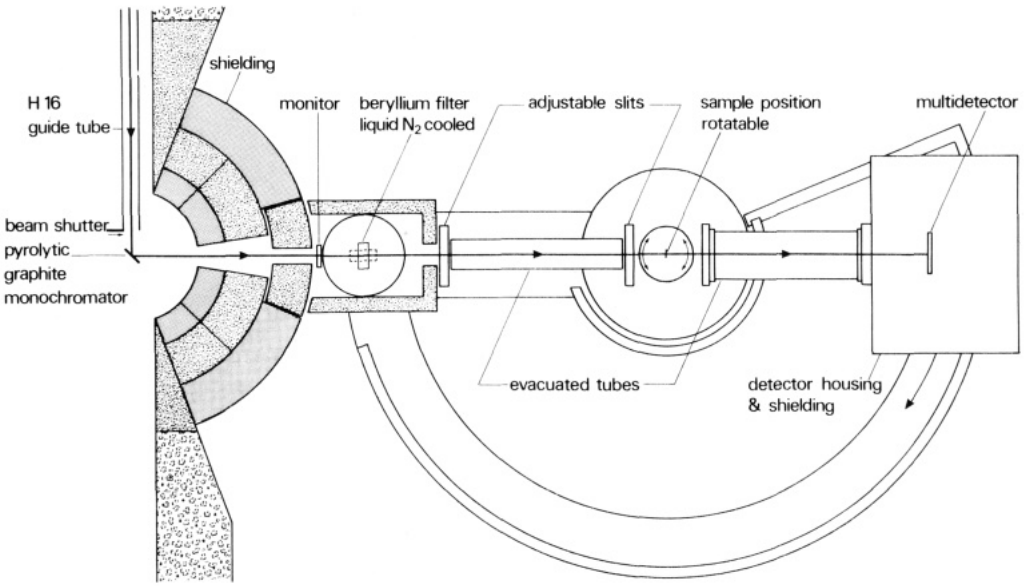

FIGURE 1: D16 neutron diffractometer installed on the H16 cold source guide at the high flux reactor of the Institut Laue-Langevin, Grenoble, France. The diagram is to scale with a sample to detector distance of 100 cm (Wilson, Braganza, and Zaccai, private communication).

The deuterium oxide (D_2O) used in the experiments was of 99.8% isotopic purity.

Multilamellar Vesicle Dispersions. Multilamellar vesicles were prepared by the usual procedure: the solvent from a chloroform/phospholipid solution containing about 45 mg of lipid in a 50-mL round-bottom flask was removed on a rotary evaporator, and MLVs were prepared by adding D_2O buffer solution (5 mM Tris, 5 mM KCl, 125 mM NaCl, pD 7.5) to the residue and shaking vigorously for 10 min above the lipid-phase transition temperature, T_m. The MLV dispersions used in the experiments contained 20 mg of lipid/mL of D_2O buffer solution.

Oriented Multilayers. For lamellar diffraction experiments, oriented samples on quartz slides were obtained by slow evaporation of solvent from solutions containing approximately 10 mg of lipid. The solvent used was 80% ethanol–20% water and the evaporation carried out above T_m of the lipid (Worcester, 1976). The quartz slides used were 32 mm by 10 mm and 0.3 mm in thickness, with the lipid covering an area of about 25 mm by 7 mm. Samples for wide-angle diffraction from the deuteriocarbon chains were prepared by the same method but with 20 mg of lipid being deposited on a 7 mm by 7 mm quartz slide.

Pressure Cell. The pressure cell used for the diffraction experiments has been described previously (Neilson et al., 1979) and was fabricated from a titanium–zirconium alloy whose constituent atoms have a mean coherent scattering amplitude of zero. This "null matrix" alloy scatters neutrons mostly incoherently and contributes no structural information to the diffracted neutron spectrum of the sample. The cylindrical pressure cell, rated for 2 kbars, has an inner diameter and height of 10 mm and 60 mm, respectively, with a wall thickness of 2.5 mm. The pressure-transmitting fluid was light machine oil with the oil–D_2O interface at the top of the cell, pressure being applied by means of a hand pump and recorded on a Budenberg gauge. Temperature was regulated by placing the cell in an aluminum block thermostated by circulating water with appropriate apertures for the incident and diffracted neutron beams. A NiCr/NiAl thermocouple placed between the aluminum block and pressure cell was used to monitor the temperature. The diffractometer slit geometry was arranged such that the neutron beam was incident only on the lower half of the cell.

MLV preparations were placed directly into the pressure cell and covered by a hollow, cylindrical Teflon piece 27 mm long, sealed at the upper end except for a central pinhole and having apertures cut out for the incident and diffracted beams. This served to isolate the sample in the neutron beam from the aqueous–oil interface at the top of the pressure cell and allowed the samples to be stirred by means of a small magnetic stirrer in the bottom of the cell.

For the oriented lipid multilayers a second quartz slide was placed over the exposed sample surface to prevent lipid being removed when immersed in D_2O in the pressure cell. The slide assembly was held vertically in the cell by means of two small cylindrical aluminum end pieces. The oriented samples for wide-angle chain diffraction measurements were laid horizontally on top of a hollow aluminum cylinder placed in the pressure cell. After samples had been mounted, the cell was filled with D_2O and connected to the oil line.

Neutron Diffractometer. The neutron diffraction experiments were carried out on the D16 neutron diffractometer installed on the H16 cold source guide at the high flux reactor of the Institut Laue-Langevin, Grenoble, France. A schematic diagram of the instrument is shown in Figure 1.

A pyrolytic graphite monochromator with a mosaic spread of 1.33° selects neutrons of wavelength 4.52 Å (wavelength spread $\Delta\lambda/\lambda \simeq 2\%$) and a liquid nitrogen cooled beryllium filter which has a cutoff at $\lambda = 3.95$ Å adequately removes contamination by higher harmonics ($\lambda/2$, $\lambda/3$, etc.). A low-efficiency neutron counter placed before the beryllium filter monitors the number of incident neutrons.

Collimation was provided by a pair of slits mounted on an optical bench, and the neutron beam size used was typically 8 mm wide and 20 mm high. An evacuated cylinder was placed between the slits to minimize air scattering. The flight path after the sample was also evacuated.

The ^3He gas multidetector which is 16 cm wide and 8 cm high consists of 64 vertical and 16 horizontal wires. This corresponds to a wire spacing of 2.54 mm horizontally and 5.08 mm vertically. The detector is scanned about the ω axis (sample rotation) with the scattering angle defined as 2θ. A sample to detector distance of 100 cm was used. At this distance, the detector subtends an angle of 9.200° at the ω axis in the horizontal plane and 4.600° in the vertical. Its angular resolution (wire spacing) is 0.145° and 0.290° in the

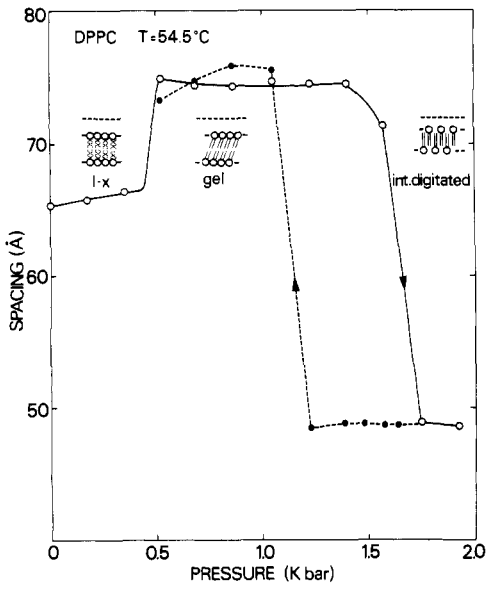

FIGURE 2: First-order Bragg spacing as a function of increasing pressure (○) and decreasing pressure (●) for DPPC MLVs in D_2O buffer solution at 54.5 °C. Also shown are schematic drawings of the different structural phases with circles representing the lipid head groups and straight and undulating lines ordered and disordered chains, respectively. l-x, liquid crystalline; int. digitated, interdigitated.

horizontal and vertical directions, respectively. The scattering vector, or Q range of the instrument, is 0.03–2.30 Å^{-1} [$Q = (4\pi \sin \theta)/\lambda$].

Data Analysis. Bragg d spacings were calculated according to the relation $n\lambda = 2d \sin \theta_n$ where n refers to the diffraction order, λ is the neutron wavelength, and θ_n the Bragg angle of the nth order which is half the angle between the incident beam and the peak center. The repeat unit for MLVs and oriented multilayers is made up of a lipid bilayer and a D_2O region.

For oriented multilayers that are centrosymmetric structures, the coherent scattering amplitude density $\rho(x)$ across the unit cell is a Fourier cosine series given by

$$\rho(x) = \sum(\pm)|F_n| \cos (2\pi nx/d)$$

where $|F_n|$ is the structure factor of the nth diffraction order with a plus or minus sign being used depending on whether the phase of the reflection is 0 or π. The structure factors were calculated from the diffraction intensities, I_n, according to

$$|F_n| = [[\sin (2\theta_n)]I_n]^{1/2}$$

where $\sin 2\theta_n$ is the Lorentz factor (Arndt & Willis, 1966).

Results

Multilamellar lipid vesicle dispersions in D_2O buffer solution gave a single intense first-order Bragg peak which was measured for 5 min at each pressure. Figure 2 shows the change in d spacing as a function of pressure up to 2.0 kbars for DPPC MLVs in D_2O buffer solution at 54.5 °C. Since T_m occurs at 42.0 °C for DPPC MLVs, at 54.5 °C the bilayers are in the liquid-crystalline state with disordered hydrocarbon chains. T_m increases with pressure, and at 54.5 °C the main transition is observed at about 0.5 kbar as an abrupt spacing increase due to hydrocarbon chain ordering. A small decrease in spacing is observed upon further increasing the pressure to 1.5 kbars where a large decrease to 49.0 Å occurs. On reducing pressure substantial hysteresis occurs since the return to the gel state is observed at $\simeq$1.2 kbars, but no hysteresis occurs at the main transition within the accuracy of the pressure measurement (±20 bars).

Temperature studies of DPPC at ambient pressure show that, in addition to the main gel–liquid-crystalline phase transition at 42.0 °C, a pretransition occurs at 34.0 °C (Hinz & Sturtevant, 1972) which corresponds to the appearance of a rippled phase (Janiak et al., 1976; Luna & McConnell, 1977) with the onset of long axis molecular rotation (Watts & Marsh, 1981; Westerman et al., 1982; Boroske & Trahms, 1983).

Spacing measurements of DPPC MLVs in D_2O buffer solution as a function of temperature show the pretransition as a gradual increase in d spacing which commences at 33.0 °C with a sharp increase at 36.5 °C (data not shown). Between 36.5 and 42.0 °C a small decrease in spacing is observed with a sharp spacing decrease at 42.0 °C corresponding to the gel–liquid-crystalline phase transition. It is evident from Figure 2 that in isothermal pressure experiments the pretransition is not observed, indicating that no appreciable volume change takes place at this transition. A similar result has been obtained for DMPC and DPPC MLVs from polarization fluorometric studies under pressure (Chong & Weber, 1983). Raman measurements, however, appear to detect a pressure-induced pretransition for DMPC (Wong et al., 1982).

Diffraction measurements from oriented multilayers of DPPC with deuteriocarbon chains immersed in D_2O in the pressure cell were made under several conditions of temperature and pressure by using the ω–2θ mode of diffraction (Arndt & Willis, 1966). In the gel state at 19.0 °C and ambient pressure, the sample was well oriented with a mosaic spread of $\simeq$3° and gave four orders of diffraction. In the liquid-crystalline state at 53.0 °C and 0.04 kbar, the mosaic spread was $\simeq$1°, and four diffraction orders were obtained; at 53.0 °C and pressures of 1.05 and 1.90 kbars, three orders were observed.

The relative phases in the presence of D_2O for multilayers of DPPC with deuteriocarbon chains have been previously determined (D. L. Worcester, unpublished data)[2] by using different saturated salt solutions to vary the relative humidity in a sealed sample container and hence change the D_2O content between bilayers so that the continuous Fourier transform of the centrosymmetric cell is sampled (Worcester, 1976). By using the phases for a sample at high relative humidity (−+++) and the structure factors calculated from the present data, the scattering density profile shown in Figure 3a was obtained for gel-state multilayers immersed in D_2O in the pressure cell at 19.0 °C and ambient pressure. The strong minima are due to the protonated lipid head groups with regions of higher scattering density being obtained for the deuteriocarbon chains and D_2O between bilayers. Since the glycerol backbone and phosphatidylcholine moiety cannot be separately resolved in this low-resolution Fourier profile, the distance between head-group minima was taken as a measure of the bilayer thickness from head-group center (phosphate group) to head-group center (phosphate group) and is 45 ± 2 Å. Taking a value from molecular models of phosphate group to phosphate group distance of $\simeq$49 Å for two fully extended chains, a value for the chain tilt angle of 23 ± 7° is obtained. This compares well with the chain tilt angle value of $\simeq$30° for fully hydrated DPPC from X-ray diffraction measurements (Tardieu et al., 1973).

Oriented multilayers immersed in D_2O in the pressure cell are fully hydrated, and the method of relative phase determination by "swelling" experiments is therefore not applicable in pressure studies. Phase determination by exchanging light water for heavy water (Worcester, 1976) is also impracticable

[2] Data collected on the small-angle scattering diffractometer at the Harwell reactor PLUTO, Atomic Energy Research Establishment, Harwell, Berkshire, U.K.

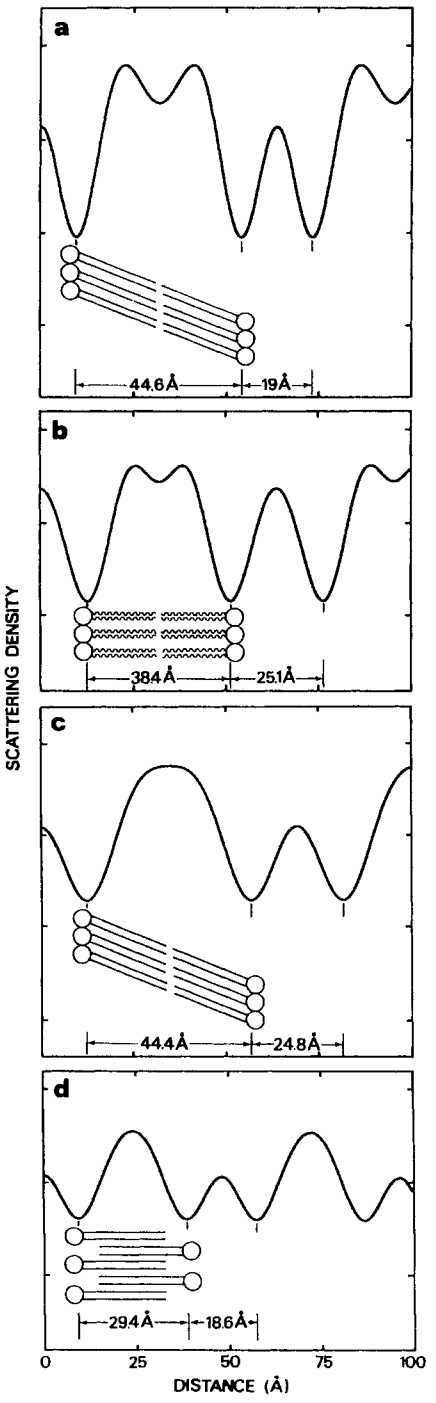

FIGURE 3: Scattering density profiles for oriented DPPC multilayers with deuteriocarbon chains in D_2O in the pressure cell at various pressures and temperatures. Schematic representations of the structures are shown beneath each profile. (a) Gel phase: T = 19.0 °C, ambient pressure, and d = 63.6 Å. (b) Liquid crystalline phase: T = 53.0 °C, P = 0.04 kbar, and d = 63.5 Å. (c) Pressure-induced gel phase: T = 53.0 °C, P = 1.05 kbar, and d = 69.2 Å. (d) Interdigitated phase: T = 53.0 °C, P = 1.90 kbars, and d = 48.0 Å. The phased structure factors used in the Fourier syntheses were the following: (a) −21.1, +5.2, +17.2, +3.1; (b) −11.9, +15.8, +10.8, −2.5; (c) −17.3, +13.3, +6.8; (d) −9.7, +9,8, +2.1. The uncertainties in the structure factors due to counting statistics were less than ±0.5% for the prominent peaks and increased to ±5% for the weak diffraction peaks. The distances given below each profile reflect the precision of the ruler measurement only; the accuracy is estimated to be ±2 Å.

in the pressure cell owing mainly to the high isotropic background of incoherently scattered neutrons from H_2O upon which the coherent diffraction peak intensities are not readily observable. Phase combinations have therefore to be selected from the 2^n possibilities where n is the number of diffraction orders. Since changing the sign of all the phases in any one combination results simply in an inversion of the Fourier profile and changing the sign of the odd-order phases shifts the origin from one center of symmetry (either D_2O or deuteriocarbon region) to the other, there are only 2^{n-2} independent phase combinations.

In the liquid-crystalline state at 53.0 °C and 0.04 kbar, four lamellar diffraction orders were observed, and so four independent Fourier profiles for the structure are possible. On the basis of the reasonable assumption that the head groups are adjacent to the D_2O regions, profiles were selected which gave regions of high-scattering density for the two centers of symmetry (D_2O and deuteriocarbon regions) separated by strong minima due to the protonated head groups. Two phase combinations −++− and −+++ resulted in such profiles giving a value for the bilayer thickness of $\simeq$38 and $\simeq$41 Å, respectively. Shown in Figure 3b is the profile calculated with the phases −++−. The d spacing of 63.5 Å remains unchanged from the gel-state value, but the deuteriocarbon chains are disordered and the bilayer thickness decreases to 38–41 from 45 ± 2 Å with an increase in the D_2O region from 19 ± 2 to 22–25 Å. The estimate of 38–41 Å for the bilayer thickness is in good agreement with the value obtained for DPPC in the liquid-crystalline state from previous neutron diffraction studies (Büldt et al., 1978).

Since three lamellar diffraction orders were observed at 53.0 °C and 1.05 and 1.90 kbars, two independent Fourier profiles for each of these structures are possible. In both cases, only the phase combination −++ resulted in profiles giving regions of high-scattering density for the deuteriocarbon and D_2O regions separated by strong head-group minima. The scattering density profiles at 53.0 °C and 1.05 and 1.90 kbars are shown in parts c and d of Figure 3, respectively. Figure 3c shows that, in the pressure induced gel state at 53.0 °C and 1.05 kbars, the bilayer structure is similar to that observed under ambient conditions, but the D_2O region is larger by 6 ± 3 Å. At 53.0 °C and 1.90 kbars, the 48.0-Å d spacing consists of a 29 ± 2 Å membrane region and a D_2O space of 19 ± 2 Å, suggesting that the chains are either tilted at 54° ± 3° with respect to the bilayer normal or interdigitated as shown in Figure 3d. Small differences between MLVs and oriented multilayers are evident in that the d spacings for oriented multilayers (Figure 3a–d) are a few percent lower than those observed for MLVs (Figure 2) under similar experimental conditions.

Figure 4a shows the wide-angle diffraction pattern obtained from DPPC with deuteriocarbon chains under ambient conditions of pressure and relative humidity at 19.0 °C. The sharp, symmetrical peak at a reciprocal spacing of $(4.12\ Å)^{-1}$ is characteristic of hexagonally packed, untilted chains observed for DPPC at a water content lower than 10% (Tardieu et al., 1973). The peak position at $(4.12\ Å)^{-1}$, however, is significantly smaller than the $(4.20\ Å)^{-1}$ reflection observed for hydrocarbon chains and is presumably an indication of stronger van der Waals' interactions between deuteriocarbon chains. At 50.0 °C and 2.0 kbars, a sharp, symmetrical peak is observed at $(4.02\ Å)^{-1}$ (Figure 4b), suggesting that the chains are not tilted (Tardieu et al., 1973) and therefore must be interdigitated to give a small membrane thickness. For a hexagonally packed lattice, the cross-sectional area per chain is $2d_h^2 3^{-1/2}$ where d_h is the chain spacing giving values of 19.6 and 18.7 $Å^2$ for the gel and interdigitated structures, respectively.

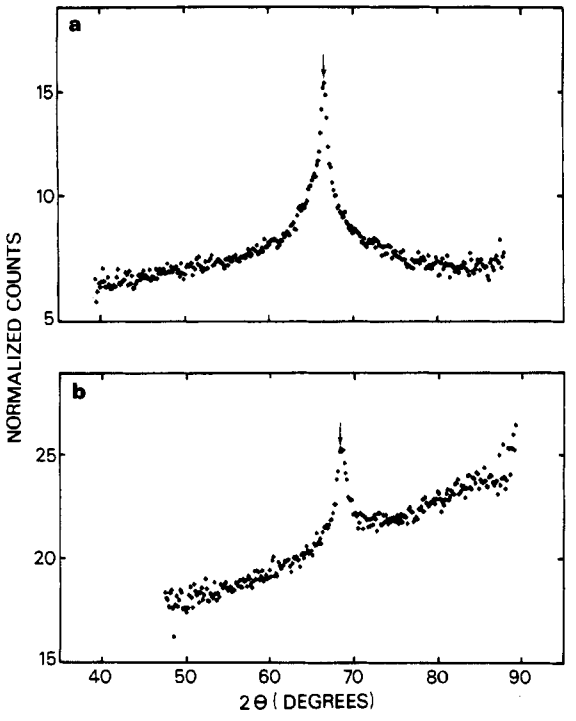

FIGURE 4: Wide-angle chain diffraction from DPPC with deuteriocarbon chains. (a) In the gel phase outside the pressure cell: ambient relative humidity and pressure, T = 19.0 °C, and d_h = 4.12 Å. (b) In the interdigitated phase: T = 50.0 °C, P = 2.0 kbars, and d_h = 4.02 Å.

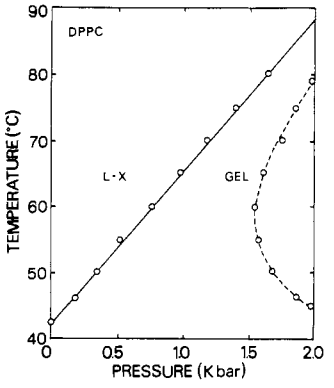

FIGURE 5: Temperature–pressure phase diagram for oriented DPPC multilayers in D_2O. The continuous line defines the liquid-crystalline–gel phase boundary and the dashed line the gel–interdigitated boundary. L-X, liquid crystalline.

The temperature–pressure phase diagrams for DPPC and DSPC in D_2O are shown in Figures 5 and 6, respectively. Measurements were made by using oriented multilayers, and phase boundaries were determined by monitoring changes in the strong first diffraction order. Pressure was increased in small steps along isotherms and followed by a 2-min measurement of the first order. The liquid-crystalline to gel transition was accompanied by an abrupt shift of the Bragg peak to lower angles due to an increase in d spacing. At the gel–interdigitated phase transition, the peak intensity decreased slowly over several minutes with the concomitant growth of intensity at higher angles corresponding to the smaller d spacing. For DSPC, the interdigitated-phase d spacing was 51.0 Å. The minimum pressure at which interdigitation occurs is clearly dependent on hydrocarbon chain length and occurs at $\simeq$0.88 and $\simeq$1.55 kbars for DSPC and DPPC, respectively. No interdigitated phase was observed for DMPC multilayers between 20 and 70 °C over a 2-kbar pressure range, but the

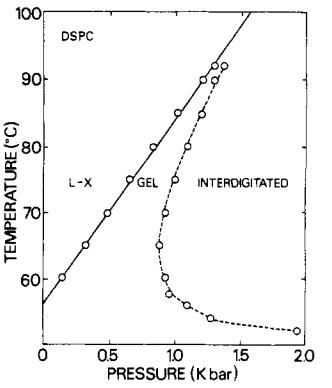

FIGURE 6: Temperature–pressure phase diagram for oriented DSPC multilayers in D_2O. L-X, liquid crystalline.

phase diagrams for DSPC and DPPC indicate that hydrocarbon chain interdigitation may occur for DMPC above 2 kbars.

The liquid-crystalline to gel transition temperature T_m increases linearly with pressure in accordance with the Clausius–Clapeyron relationship, and the dT_m/dP values calculated from the phase diagrams are 28.0 °C/kbar for DSPC and 23.0 °C/kbar for DPPC and DMPC. These values are in good agreement with those previously determined for DPPC and DMPC MLVs (Chong & Weber, 1983).

Discussion

Biological membranes and lipid bilayers in the liquid-crystalline state are laterally compressible so that pressure increases chain order by reducing the cross-sectional area occupied per hydrocarbon chain while temperature exerts the opposite effect and causes disordering. This allows a temperature to pressure equivalence dT/dP to be defined in terms of membrane fluidity and is the decrease in temperature required to achieve the same reduction in fluidity as a given unit increase of pressure (usually 1 kbar). Membranes from synaptic and myelin fractions of goldfish brain given dT/dP values around 13–19 °C/kbar (Chong & Cossins, 1983) with a value of 21 °C/kbar being obtained for lipid bilayers in the liquid-crystalline state (Chong & Weber, 1983).

For single-component phospholipid bilayers that exhibit a gel to liquid-crystalline phase transition, the transition temperature T_m increases linearly with pressure. Values of dT_m/dP for DMPC, DPPC, and DSPC were obtained that fall within the 15–30 °C/kbar range of values reported in the literature for synthetic phospholipids (Trudell et al., 1974; Liu & Kay, 1977; Ceuterick et al., 1978; Mountcastle et al., 1978). The existence of an isothermal pressure induced gel to interdigitated hydrocarbon chain phase transition illustrates that dT_m/dP values for DPPC and DSPC can only be interpreted as the temperature to pressure equivalence in terms of constant membrane fluidity or order (Chong & Weber, 1983) over that part of the phase diagram where the bilayer remains in a liquid-crystalline state and for a limited range of temperatures and pressures in the gel phase.

In contrast to the liquid-crystalline–gel transition, the pressure induced gel to interdigitated phase transition is highly time dependent and exhibits strong hysteresis (Figure 2). The shortest time over which the transition occurs at a constant pressure is approximately 5 min, this time increasing with decreasing temperature and so making the onset of the pressure-induced interdigitated phase difficult to judge at the lower temperatures. A curved temperature–pressure phase boundary exists between the gel and interdigitated phases (Figures 5 and 6), and for a range of pressures, raising the

temperature from the gel phase results first in the transition to the interdigitated phase followed by a transition back to the gel phase at higher temperatures. Qualitatively, the curved phase boundary is explained by the strong van der Waals' interaction energy between ordered chains at low temperature in the gel phase and the increase in entropy or chain disorder at high temperature so that the free energy of the interdigitation of chains from apposing monolayers passes through a broad minimum enabling interdigitation to occur at lower pressures in the intermediate temperature range. A similar explanation in molecular terms has been given by Weber and Drickamer (1983) for the curved boundaries observed in the pressure–temperature phase diagrams between the native and denatured states of proteins (Brandts et al., 1970; Hawley, 1971; Zipp & Kauzmann, 1973).

The transition to the interdigitated phase occurs in response to applied pressure because interdigitation results in a smaller hydrocarbon volume due to the $\simeq$5% decrease in cross-sectional area occupied per chain on going from the gel to interdigitated phases. Since the molar volumes of hydrocarbons in dilute aqueous solution are smaller than in nonpolar solvents (Masterton, 1954), a further volume decrease may be occurring if the hydrocarbon chain terminal methyl groups are becoming exposed to water. In energy terms, the more efficient packing in the interdigitated phase results in an increased van der Waals' chain interaction energy. However, energy is lost when the terminal methyl groups become exposed to water, while the expansion of the head-group lattice also results in an energy reduction due to weaker lateral head-group interactions (Simon & McIntosh, 1984).

The minimum pressure at which interdigitation occurs decreases with increasing chain length. This is clearly a consequence of the expected larger decrease in hydrocarbon volume per mole of lipid and the larger energy gain from van der Waals' interactions when longer chains interdigitate, so that it becomes favorable for longer chains to interdigitate at lower pressures. The difference between the minimum pressures where interdigitation occurs for DPPC ($C_{16:0}$) and DSPC ($C_{18:0}$) is $\simeq$0.7 kbar, suggesting that the lowest pressure at which DMPC ($C_{14:0}$) chains will interdigitate is $\simeq$2.2 kbars.

Structurally similar interdigitated phases have been observed for fully hydrated 1,2-dipalmitoyl-*sn*-glycero-3-phosphatidylglycerol (DPPG) bilayers (Ranck & Tocanne, 1982a,b) and DPPC bilayers (McIntosh et al., 1983; Simon & McIntosh, 1984) in the presence of small surface active molecules and for fully hydrated 1,3-dipalmitoyl-*sn*-glycero-2-phosphatidylcholine (β-DPPC) between 30 and 35 °C (Serrallach et al., 1983).

Registry No. DMPC, 18194-24-6; DPPC, 63-89-8; DSPC, 816-94-4.

REFERENCES

Arndt, U. W., & Willis, B. T. M. (1966) *Single Crystal Diffractometry*, Cambridge University Press, Cambridge.

Boroske, E., & Trahms, L. (1983) *Biophys. J. 42*, 275–283.

Brandts, J. F., Oliviera, R. J., & Westort, C. (1970) *Biochemistry 9*, 1038–1047.

Büldt, G., Gally, H. U., Seelig, A., Seelig, J., & Zaccaï, G. (1978) *Nature (London) 271*, 182–184.

Ceuterick, F., Peeters, J., Heremans, K., De Smedt, H., & Olbrechts, H. (1978) *Eur. J. Biochem. 87*, 401–407.

Chong, P. L.-G., & Cossins, A. R. (1983) *Biochemistry 22*, 409–415.

Chong, P. L.-G., & Weber, G. (1983) *Biochemistry 22*, 5544–5550.

Hawley, S. A. (1971) *Biochemistry 10*, 2436–2442.

Hinz, H.-J., & Sturtevant, J. M. (1972) *J. Biol. Chem. 247*, 6071–6075.

Janiak, M. J., Small, D. M., & Shipley, G. G. (1976) *Biochemistry 15*, 4575–4580.

Liu, N.-I., & Kay, R. L. (1977) *Biochemistry 16*, 3484–3486.

Lown, D. A., Thirsk, H. R., & Lord Wynne-Jones (1968) *Trans. Faraday Soc. 64*, 2073–2080.

Luna, E. J., & McConnell, H. M. (1977) *Biochim. Biophys. Acta 470*, 303–316.

Masterton, W. L. (1954) *J. Chem. Phys. 22*, 1830–1833.

McIntosh, T. J., McDaniel, R. V., & Simon, S. A. (1983) *Biochim. Biophys. Acta 731*, 109–114.

Mountcastle, D. B., Biltonen, R. L., & Halsey, M. J. (1978) *Proc. Natl. Acad. Sci. U.S.A. 75*, 4906–4910.

Nielson, G. W., Page, D. I., & Howells, W. S. (1979) *J. Phys. D 12*, 901–907.

Ranck, J. L., & Tocanne, J. F. (1982a) *FEBS Lett. 143*, 171–174.

Ranck, J. L., & Tocanne, J. F. (1982b) *FEBS Lett. 143*, 175–178.

Serrallach, E. N., Dijkman, R., De Haas, G. H., & Shipley, G. G. (1983) *J. Mol. Biol. 170*, 155–174.

Simon, S. A., & McIntosh, T. J. (1984) *Biochim. Biophys. Acta 773*, 169–172.

Tardieu, A., Luzzati, V., & Reman, F. C. (1973) *J. Mol. Biol. 75*, 711–733.

Trudell, J. R., Payan, D. G., Chin, J. H., & Cohen, E. N. (1974) *Biochim. Biophys. Acta 373*, 436–443.

Watts, A., & Marsh, D. (1981) *Biochim. Biophys. Acta 642*, 231–241.

Weber, G., & Drickamer, H. G. (1983) *Q. Rev. Biophys. 16*, 89–112.

Westerman, P. W., Vaz, M. J., Strenk, L. M., & Doane, J. W. (1982) *Proc. Natl. Acad. Sci. U.S.A. 79*, 2890–2894.

Wong, P. T. T., Murphy, W. F., & Mantsch, H. H. (1982) *J. Chem. Phys. 76*, 5230–5237.

Worcester, D. L. (1976) in *Biological Membranes* (Chapman, D., & Wallach, D. F. H., Eds.) Vol. 3, pp 1–46, Academic, New York.

Zipp, A., & Kauzmann, W. (1973) *Biochemistry 12*, 4217–4228.